Selective etching of spin-coated and thermally evaporated $As_{30}S_{45}Se_{25}$ thin films

K. Palka[a,b], S. Slang[b], J. Buzek[a], M. Vlcek[b]

[a]Department of General and Inorganic Chemistry, Faculty of Chemical Technology, University of Pardubice, 532 10 Pardubice, Czech Republic

[b]Center of Materials and Nanotechnologies, Faculty of Chemical Technology, University of Pardubice, 532 10 Pardubice, Czech Republic

Abstract

Chalcogenide glasses are intensively studied materials due to their interesting optical properties such as high values of refractive index, wide transparency in IR, photosensitivity, etc. We report on the comparison of photo and thermo-induced changes in optical properties and chemical resistance of thermally evaporated and spin-coated $As_{30}S_{45}Se_{25}$ thin films. Significantly different trends of photo-induced changes in chemical resistance in both types of thin films such as negative etching of thermally evaporated thin films and positive etching of spin-coated thin films were observed. The structural changes responsible for the observed phenomena were investigated as well.

1. Introduction

Chalcogenide glasses (ChGs) are promising materials for many applications (especially in IR optics) due to their interesting physical and chemical properties such as high values of refractive index, wide transmission window in IR spectral range, frequent photosensitivity which together with good solubility in alkaline solutions often results in selective etching of ChGs, etc. [1]. Particular attention has been paid to ChGs of As-S-Se system. ChGs of this system can be prepared in wide range of glass compositions due to the broad glass forming region [2], which allows tailoring of physical and chemical properties. ChGs of As-S-Se system have been thoroughly studied as materials suitable for holography and lithography because of their significant photosensitivity resulting in selective etching in both organic and inorganic alkaline solutions [3 - 6]. Further interest in ChGs of this system was attracted because of their significant non-linear optical properties [7 - 9] and the possibility of photo-doping with Ag [10, 11].

Many applications of ChGs require the glass to be in a thin film (TF) form. The traditional methods of the TF deposition such as vacuum thermal evaporation, sputtering and PLD form the TF from the gaseous phase [12, 13]. Alternatively the TFs can be prepared from the solution of ChG in volatile alkaline solvent. Methods such as spin-coating [14] and spiral bar coating [15] can be used for a TF deposition. The advantages of solution based deposition methods lie in the simplicity of the techniques (no need for high vacuum) and in the possibility to use well managed coating techniques for TF deposition [15]. On the other hand the TFs prepared via solution contain residual amount of the solvent captured in their structure, which can alter the physical and chemical properties of the glass [16].

We report on the comparison of $As_{30}S_{45}Se_{25}$ TFs prepared using thermal evaporation and spin-coating. The optical properties, chemical resistance, structure and their photo and thermo-induced changes were investigated and discussed in dependence on the method of the TF deposition.

2. Experimental details

The source bulk glass was prepared by standard melt quenching method. The high purity (5N) elements were loaded into cleaned quartz ampoule in appropriate amounts. The ampoule was consequently evacuated (~ 10^{-3} Pa) and sealed. The synthesis was performed in rocking tube furnace at 850°C. Quenching was done in cold water. Obtained bulk glass was used for TF deposition using thermal evaporation and spin-coating.

Thermal evaporation was carried out using device UP-858 (Tesla, Czech Republic). The residual pressure during TF deposition was ~10^{-3} Pa. Evaporation rate as well as the thickness of deposited TF was measured *in situ* during deposition by quartz crystal microbalance method. The evaporation rate

was ~1 nm.s^{-1}. Thickness of deposited TF was ~ 185 nm in order to be similar to the thickness of as-prepared spin-coated TFs.

Source bulk glass was manually powdered and dissolved in n-butylamine (BA) for purposes of spin-coating. TFs were prepared using spin-coater SC110 (Best Tools, USA) onto cleaned silicate glass substrates. Freshly prepared TFs were stabilized by annealing at 60°C for 20 minutes in order to remove the excess solvent.

TFs prepared by both used methods were stored in dark dry environment at laboratory temperature.

Annealing of TFs was performed using annealing table (Conbrio, Czech Republic) providing homogeneous thermal field over the whole surface of the samples. Annealing at temperatures 80 and 100°C was performed for 60 minutes in protective Ar atmosphere in order to prevent surface oxidation. The annealing temperatures were chosen with respect to the decomposition temperatures of salts (glass dissolving products) inside the matrix of spin-coated TFs (70-90°C) and still below the T_g of ChGs with the similar compositions [14, 16]. As-prepared and annealed TFs were exposed to the solid state green laser beam (532 nm ~ 2.33 eV, 380 mW.cm^{-2}; Roithner Lasertechnik, Austria) for 60 minutes in protective Ar atmosphere.

Transmission spectra of studied TFs were measured using spectrometer UV-3600 (Shimadzu, Japan). Structure of the TFs was investigated by Raman spectroscopy using FTIR spectrometer IFS 55 with Raman accessory FRA 106 (Bruker, Germany). Nd:YAG laser (λ = 1064 nm) was used as an excitation beam. Presented Raman spectra were normalized by the intensity of the most intensive band in the spectrum.

The kinetics of TFs dissolution in BA based solution in aprotic solvent were measured and evaluated by procedure described in [17].

3. Results and discussion

3.1 Methodology of transmission spectra evaluation

Optical parameters of TFs were determined from measured transmission spectra. Thickness (*d*) and spectral dependence of refractive index (*n*) were calculated from transparent region (extinction coefficient $k \rightarrow 0$) of measured transmission spectra by fitting a model of transmission spectrum (Fig. 1) presented by Swanepoel [18] where absorption in the TF is neglected (k = 0) and dispersion of refractive index *n* is expressed by Wemple-DiDomenico's equation [19]:

$$n^2 - 1 = \frac{E_d E_0}{E_0^2 - (h\nu)^2} \quad (1),$$

where E_d is parameter of dispersion energy, E_0 is single oscillator energy and $h\nu$ is photon energy. Described evaluation method is suitable for very thin films of dielectric materials [15] when the measured transmission spectra exhibit insufficient number of interference fringes for classical Swanepoel's method to be used.

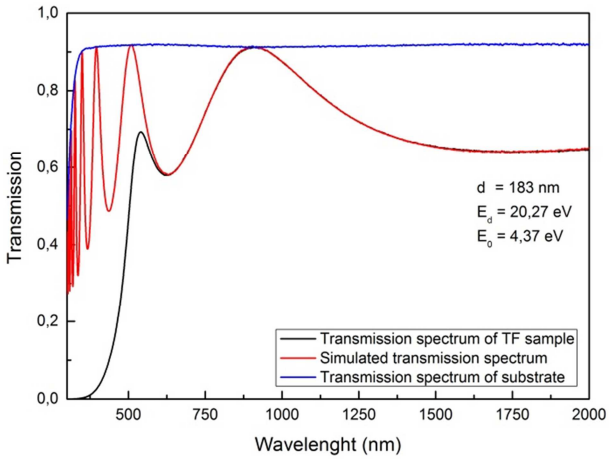

Fig. 1. The transmission spectrum of thermally evaporated $As_{30}S_{45}Se_{25}$ TF (black) and silicate glass substrate (blue) together with the fitted transmission spectrum (red).

The values of absorption coefficients α were calculated from measured transmission spectra using procedure described in [18]. The optical bandgap values E_g^{opt} of TFs were determined by Tauc's method for semiconductors [20].

Optical properties of both thermally evaporated and spin-coated TFs were measured on four separate samples for each treatment in order to increase the accuracy of the measurements. The error bars presented in the following plots represent the standard deviation of measured values.

3.2 Optical properties

Refractive index of as-prepared thermally evaporated TFs was 2.44 at 1064 nm (Fig. 2A). Annealing of the samples at 80 and 100°C for 1h did not influence this value significantly. Exposure to the beam of 532 nm laser (380 mW.cm^{-2}) for 1 h caused increase of the refractive index to the value 2.51. This value did not differ for any of the annealed samples. The optical band gap (E_g^{opt}) of as-prepared thermally evaporated TFs was 2.00 eV (Fig. 2B). Annealed samples exhibited increase of E_g^{opt} to the value 2.03 eV for the sample annealed at 80°C and 2.04 eV for the sample annealed at 100°C. Exposure of the as-prepared thermally evaporated TFs did not cause any change of the E_g^{opt}. Both annealed samples exhibited photo-darkening (red shift) after exposure to the laser beam dropping the value of the E_g^{opt} to 2.00 eV. The thicknesses of the annealed thermally evaporated samples increased slightly with increasing temperature of the annealing (Fig. 2C). Exposure of the as-prepared and annealed samples to the laser beam resulted in slight compression (~3 nm) of the TFs (Fig. 2C). All of the changes in the thicknesses of the evaporated TFs are on the verge of the evaluation method's preciseness; nevertheless the trend is apparent (Fig. 2C).

Refractive index of as-prepared spin-coated TFs was 2.13 at 1064 nm (Fig. 2D), which is significantly lower value in comparison with the TFs prepared by thermal evaporation (Fig. 2A). The difference in the values of refractive index is most likely caused by residual amount of BA enclosed in the structure of the spin-coated samples [16]. Annealing of the as-prepared spin-coated TFs at 80 and 100°C respectively caused partial release of the solvent from the TF resulting in the increase of refractive index up to the value 2.26 for the sample annealed at 100°C. The exposure of the samples prepared by spin-coating to the 532 nm laser beam does not cause any significant change in the values of refractive index in as-prepared and 80°C annealed TF. Sample annealed at 100°C exhibits photo-induced increase of the refractive index to the value 2.29 (at 1064nm).

The E_g^{opt} of the as-prepared spin-coated TFs was 1.91 eV (Fig. 2E). This value is slightly lower that E_g^{opt} of thermally evaporated samples. Annealing of the as-prepared spin-coated TFs at 80 and 100°C increased the value of the E_g^{opt} to 1.97 eV, which is comparable with the values of thermally evaporated TFs' E_g^{opt} (Fig. 2B). Exposure to the 532 nm laser beam caused photo-bleaching (blue shift) of the as-prepared spin-coated samples increasing the value of E_g^{opt} to 1.94 eV. Contrary to the exposure of as-prepared TFs the exposures of annealed samples (both 80 and 100°C) caused photo-

darkening. In case of the sample annealed at 80°C the optical band gap decreased to 1.91 eV and 1.94 eV for the sample annealed at 100°C.

The thickness (*d*) of spin-coated TFs depends significantly on the thermal history of the sample (Fig. 2F). The thickness of as-prepared spin-coated TFs was ~ 185 nm. The thickness of annealed samples decreased significantly - *d* = 160 nm in case of the TFs annealed at 80°C and *d* = 155 nm in case of the samples annealed at 100°C. With increasing temperature of annealing the thickness decreases due to the release of solvent molecules bonded within the structure of TF [16, 21]. Exposure to the 532 nm laser beam induces no significant changes in the thickness of any studied spin-coated TF.

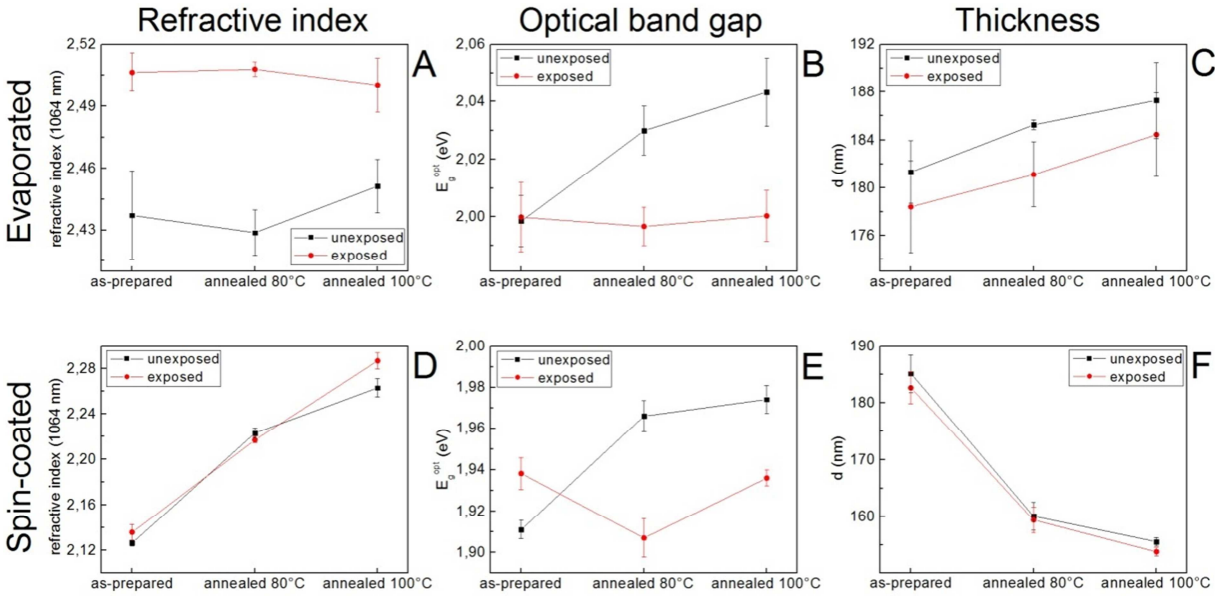

Fig. 2. Optical properties of thermally evaporated and spin-coated $As_{30}S_{45}Se_{25}$ TFs.

3.3 Etching kinetics

Both thermally evaporated and spin-coated TFs were etched in solution of BA in aprotic solvent. Thermally evaporated TFs proved to be significantly more resistant in comparison with spin-coated TFs. Thus concentration of BA in solutions used for etching of thermally evaporated TFs was 1 vol.% and 0.1 vol.% concentration was used for etching of spin-coated TFs. Measured etching curves are presented in Fig. 3. The etching curves consists of only three points due to the very low thickness of studied TFs (<200 nm). On account of credibility the presented plots of etching curves are supplied with inset graphs showing the dependence of the transmission related to the wavelength of the first interference maximum in the transmission spectrum on the time of etching (Fig. 3).

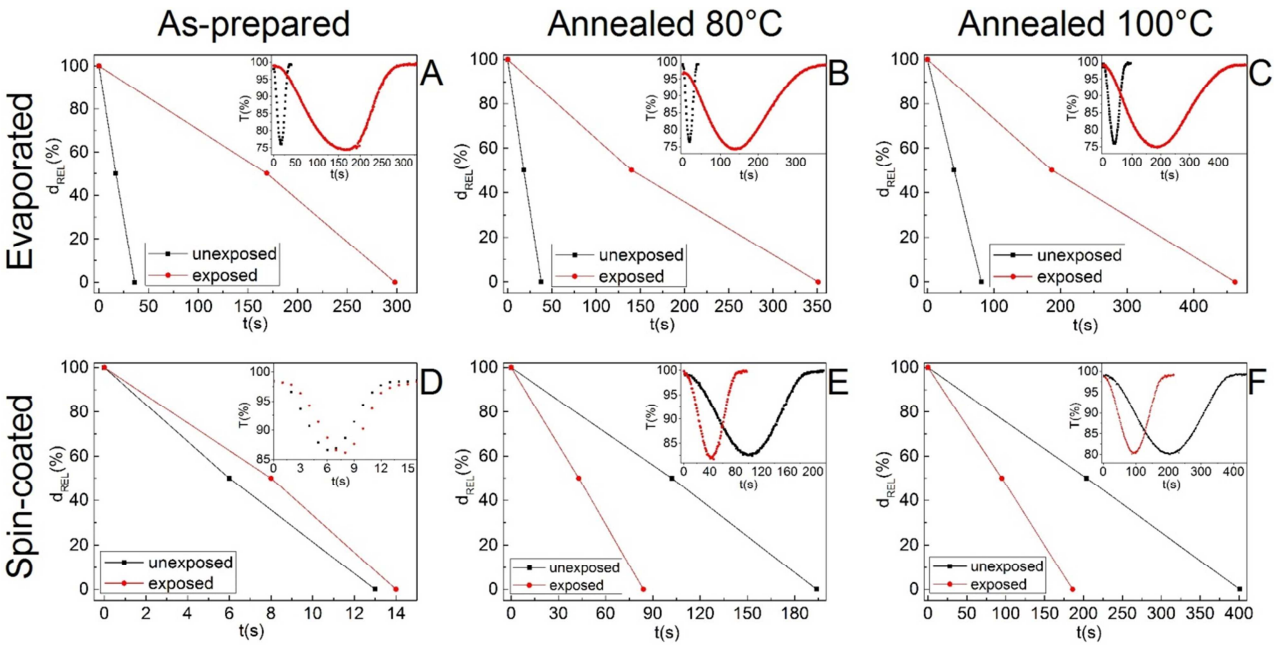

Fig. 3. Etching curves of thermally evaporated and spin-coated $As_{30}S_{45}Se_{25}$ TFs. The insets show the dependence of the intensity related to the wavelength of the first interference maximum in the transmission spectrum on the time of etching.

The average etching rates *W* were calculated using the values of TFs thicknesses obtained by the evaluation of TFs transmission spectra and the times needed for complete dissolution of TFs (Fig. 4).

The etching rates of the samples prepared by thermal evaporation (Fig. 4A) show that as-prepared and 80°C annealed sample dissolve at similar rate. Sample annealed at 100°C exhibits significantly lower etching rate due to the partial relaxation of the glass structure caused by annealing (see below the discussion on TF's structure). Significant decrease of the etching rate occurs after the exposure to 532 nm laser beam for both as-prepared and annealed samples. Decrease of the etching rate in the exposed parts of the TF results in negative etching (exposed areas dissolve at lower rate than unexposed areas).

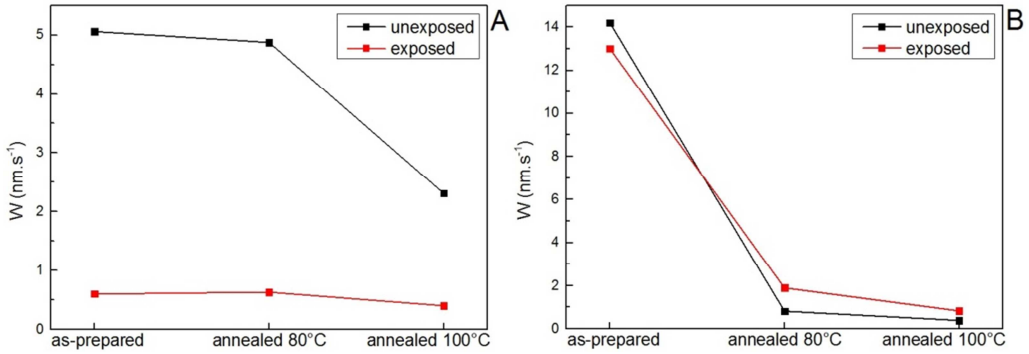

Fig. 4. The average etching rates W of thermally evaporated (A) and spin-coated (B) TFs in BA based solution.

Fig. 4B gives evidence of very high etching rates for both unexposed and exposed as-prepared spin-coated TFs. The etching rate of exposed TFs is slightly lower than etching rate of unexposed TF. Nevertheless due to the high etching rate and 1 s sampling period during the measurement (Fig. 3D inset) the difference between etching rate of exposed and unexposed TFs is on the verge of the method's preciseness.

The etching rates of annealed spin-coated TFs exhibit significantly different trends comparing with the as-prepared TFs. The etching rates of unexposed annealed spin-coated TFs are significantly

lower (well below 1 $nm.s^{-1}$) (Fig. 4B). Thus even low temperature annealing causes significant increase in chemical resistance. The etching rate decreased 17 times in case of the sample annealed at 80°C and 36 times for the sample annealed at 100°C in comparison with the etching rate of as-prepared TF.

Exposure to the 532 nm laser beam induces significant increase in the etching rate of annealed spin-coated TFs (Fig. 4B). In case of 80°C annealed sample the etching rate increases from 0.8 $nm.s^{-1}$ to 1.9 $nm.s^{-1}$; and for 100°C annealed sample from 0.4 to 0.8 $nm.s^{-1}$. The photo-induced increase of the etching rate is completely opposite to the observed photo-induced changes of the chemical resistance of thermally evaporated TFs and results in positive etching (exposed areas dissolve at higher rate than unexposed areas) contrary to the negative etching of thermally evaporated TFs.

In order to demonstrate the selectivity of the etching process even in low temperature (80°C) annealed spin-coated TFs a diffraction grating with period 20 μm was prepared using selective etching method. The exposure of the grating motive was done through the chromium mask by contact method. The exposure was carried out with the same parameters as other exposures described in this paper (532 nm laser beam, 380 $mW.cm^{-2}$, exposure time 1 h). The quality of prepared grating was investigated using optical microscopy (Fig. 5).

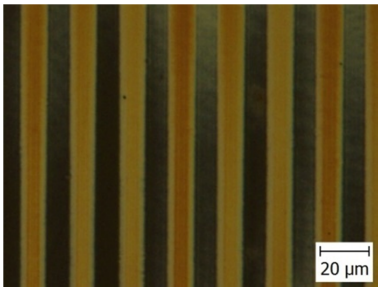

Fig. 5. Diffraction grating prepared in spin-coated pre-annealed $As_{30}S_{45}Se_{25}$ TF by selective etching.

3.4 Raman Spectra

The interpretation of observed changes of optical parameters and chemical resistance are supported by knowledge of structural changes occurring during annealing and exposure of both thermally evaporated and spin-coated TFs. The Raman spectrum of source bulk $As_{30}S_{45}Se_{25}$ ChG together with the Raman spectra of as-prepared, annealed and exposed TFs deposited by thermal evaporation and spin-coating are presented in Figs. 6 and 7 respectively. The Raman spectrum of source bulk ChG confirms that the dominant structural units of studied glass composition are $AsS_{3/2}$ pyramidal units with the bands at 342 and 380 cm^{-1} [22 - 25]. In addition, the structure of source bulk ChG comprises of $AsSe_{3/2}$ pyramidal units (shoulder at 230 cm^{-1} [26 - 29]), Se_8 rings with the band at 258 cm^{-1} [7, 27, 28, 30], S_8 rings (475 cm^{-1} [7, 23, 26, 31]) and S–S chain fragments (495 cm^{-1} [7, 28, 31, 32]).

The Raman spectra of thermally evaporated TFs (Fig.6) proved that in comparison with the structure of the source bulk glass, the structure of as-prepared thermally evaporated TF is significantly different and highly disordered. The dominant structural units of as-prepared thermally evaporated TFs are the $AsSe_{3/2}$ and $AsS_{3/2}$ pyramidal units (well-developed bands at 230 and 342 cm^{-1}, respectively). The intensity of $AsSe_{3/2}$ pyramidal units' band at 230 cm^{-1}, seen only as a shoulder in the Raman spectrum of source bulk glass, now distinctly overlaps the intensity of Se_8 rings' band at 258 cm^{-1}. The intensity of S–S chain band at 495 cm^{-1} is also higher. Two additional bands at 220 (minor shoulder) and 362 cm^{-1} appear in Raman spectrum of as-prepared thermally evaporated TFs. These bands can be attributed to the vibrations of arsenic rich realgar-like As_4S_4 structural units [24, 25, 29]. The small sharp bands below 200 cm^{-1} (135 and 188 cm^{-1}) can be also attributed to the vibrations of As-As homopolar bonds of the same realgar-like As_4S_4 structural units [24].

The Raman spectra of annealed evaporated TFs confirm that the thermal treatment induces structural polymerization. The level of structural polymerization increases with increasing annealing temperature and the structure of TFs shifts closer to the structure of source bulk glass. The bands

intensities of $AsSe_{3/2}$ pyramidal units (230 cm^{-1}), As_4S_4 realgar-like structural units (135, 188, 220, 362 cm^{-1}) and S–S chains (495 cm^{-1}) gradually decrease as the bands intensities of Se_8 chains (258 cm^{-1}) and $AsS_{3/2}$ pyramidal units (342 cm^{-1}) increase. Our results are in good agreement with W. Li et al. [27] concluding that in chalcogen rich As-S-Se system, the Se atoms tend to form Se–Se bonds, while S atoms prefer to form As-S bonds in $AsS_{3/2}$ pyramidal units. The annealing time (1 h) and temperatures well below the T_g were insufficient to change the structure of thermally evaporated TF quantitatively and thus there still is an observable difference between the structure of source bulk glass and the structure of annealed thermally evaporated TF.

The laser beam exposure of thermally evaporated as-prepared and annealed TFs also induces structural polymerization similar to the process induced by annealing but the changes are more significant. The bands of As_4S_4 realgar-like structural units (135, 188, 220, 362 cm^{-1}) and S–S chains (495 cm^{-1}) practically disappear and the $AsSe_{3/2}$ pyramidal units' band (230 cm^{-1}) is visible only as a weak shoulder. The level of structural polymerization slightly increases with the annealing temperature of pre-annealed exposed samples, but their overall structure is very close to that of the source bulk glass.

Observed changes in the structure of thermally evaporated TFs correspond with the described changes in their chemical resistance. Photo or thermo-induced formation of Se_8 rings together with $AsS_{3/2}$ polymerization significantly increases the chemical resistance of the TFs resulting in the drop of the etching rate (Fig. 4A). The increase of chemical resistance of thermally evaporated TFs is probably connected with insolubility of elemental Se in BA [33, 34].

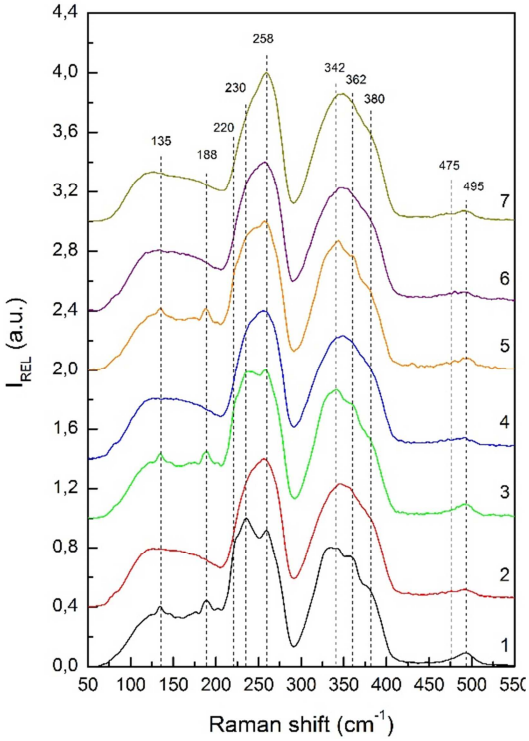

Fig. 6. Raman spectra of thermally evaporated TFs. 1: as-prepared TF; 2: as-prepared exposed TF; 3: TF annealed at 80°C; 4: TF annealed at 80°C and exposed; 5: TF annealed at 100°C; 6: TF annealed at 100°C and exposed; 7: source bulk glass. For treatment details see Experimental details section.

The Raman spectra of as-prepared, annealed and exposed spin-coated TFs (Fig. 7) prove that the structure of spin-coated TFs is very similar to the structure of the source bulk glass. Similar observations have been previously reported on related As-S system [21, 35]. The most intensive bands in the Raman spectrum of as-prepared spin-coated TF can be attributed to the vibrations of Se_8 rings (258 cm^{-1}), $AsS_{3/2}$ pyramidal units (342 cm^{-1}) and As_4S_4 realgar-like structural units (369 cm^{-1}). It should be noted that the band intensity of As_4S_4 realgar-like structural units at 369 cm^{-1} slightly

overlaps the intensity of $AsS_{3/2}$ pyramidal units' band at 342 cm^{-1} and its position is shifted from 362 to 369 cm^{-1}, which was also reported in Raman spectra as-prepared As-S spin-coated TFs of sulfur rich compositions [13, 21, 35]. The bands corresponding to the vibration of S_8 rings (475 cm^{-1}) and S–S chains (495 cm^{-1}) are also present in the measured Raman spectrum of as-prepared spin-coated TF. An additional band at 415 cm^{-1} can be found in the Raman spectra of spin-coated TFs (Fig. 7) (missing in Raman spectra of thermally evaporated TFs). This band can be attributed to the vibrations of alkyl ammonium arsenic sulfide salts (AAAS salts) produced during dissolution of source bulk As-S glasses in aliphatic amines [16, 21, 35]. Similarly to the thermally evaporated TFs, the spin-coated TFs also undergo structural polymerization during thermal treatment, but the nature of these changes is quite different. With the increase of annealing temperature the band intensities related to the vibrations of Se_8 rings (258 cm^{-1}), As_4S_4 realgar-like structural units (369 cm^{-1}), AAAS structural units (415 cm^{-1}), S_8 rings (475 cm^{-1}) and S–S chains (495 cm^{-1}) decrease as the intensities of bands in the region 230-250 (mixed As-S-Se pyramidal units [7, 26, 27, 28]) and 342 cm^{-1} ($AsS_{3/2}$) increase. Thermal treatment induces decomposition of AAAS connected with the releasing of residual solvent molecules. According to the Kohoutek and Chern [14, 16] these salts decompose bellow 90°C and thus annealing at 100°C decreases their concentration significantly. Decomposition process is accompanied by the polymerization of different sulfuric structural units (S_8 rings, S-S chains and single coordinated S originated from AAAS decomposition [35]), Se_8 rings and arsenic rich As_4S_4 realgar-like structural units producing $AsS_{3/2}$ and mixed As-S-Se pyramidal structural units [7, 26 - 28]. The thermo-induced decomposition of AAAS together with the release of bonded BA molecules causes significant decrease in the thickness of the TFs (Fig. 2F), increase in both n and E_g^{opt} (Figs. 2D and E) and significant increase of chemical resistance (drop of the etching rate respectively) of the spin-coated TFs.

The laser beam exposure of as-prepared spin-coated TFs cause no significant changes in the TFs structure, which is in a good agreement with the observed lack of significant difference in the chemical resistance of unexposed and exposed spin-coated TFs.

The exposure of annealed spin-coated TFs induces structural changes, but their nature significantly differs from those of thermally evaporated TFs. With increasing annealing temperature of pre-exposed spin-coated TFs the intensities of the bands corresponding to the vibrations of Se_8 rings (258 cm^{-1}) and As_4S_4 realgar-like structural units (369 cm^{-1}) decrease after exposure and the intensities of mixed As-S-Se pyramidal structural units' bands increase (230-250 cm^{-1}). Thus the Se_8 rings are broken during laser beam exposure reacting with weak As-As homopolar bonds [35] in As_4S_4 realgar-like structural units and the network of mixed As-S-Se pyramidal units is formed. Observed photo-induced structural changes in annealed spin-coated TFs (opening of Se_8 rings and formation of mixed As-S-Se pyramidal units) result in decrease in the chemical resistance of spin-coated TFs. Thus positive etching was observed.

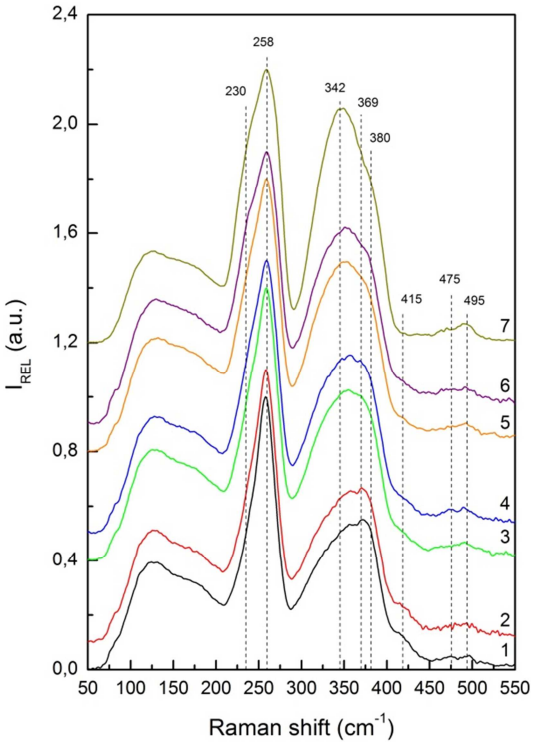

Fig. 7. Raman spectra of SC TFs. 1: as-prepared TF; 2: as-prepared exposed TF; 3: TF annealed at 80°C; 4: TF annealed at 80°C and exposed; 5: TF annealed at 100°C; 6: TF annealed at 100°C and exposed; 7: source bulk glass. For treatment details see Experimental details section.

4. Conclusions

Optical properties, chemical resistance and structure of thermally evaporated and spin-coated $As_{30}S_{45}Se_{25}$ TFs were studied and discussed. Presented results gave evidence of photo and thermo-induced changes in optical properties and chemical resistance of studied TFs. The exposure of as-prepared and annealed (80 and 100°C; 1 h) thermally evaporated TFs to the 532 nm laser beam caused significant increase in chemical resistance resulting in negative etching. Contrary the exposure of annealed spin-coated TFs resulted in positive etching. The origin of the observed phenomena was found in significant differences in photo-structural changes in thermally evaporated and spin-coated TFs investigated by Raman spectroscopy.

Acknowledgement

Authors appreciate financial support from project No. 16-13876S financed by the Grant Agency of the Czech Republic (GA CR) as well as support from the grants LM2015082 and CZ.1.05/4.1.00/11.0251 from the Ministry of Education, Youth and Sports of the Czech Republic.

References

[1] Tanaka K., Shimakawa K., Amorphous chalcogenide semiconductors and related materials, Springer 2011
[2] Borisova Z.U., Glassy Semiconductors, Plenum Press 1981
[3] Bulanovs A., Gerbreders V., Kirilovs G., Teteris J., Cent. Eur. J. Phys. 9(5) (2011) 1327-1333
[4] Orava J., Wagner T., Krbal M., Kohoutek T., Vlcek M., Frumar M., J. Non-Cryst. Solids 353 (2007) 1441-1445
[5] Stronski A.V., Vlcek M., Sklenar A., Shepeljavi P.E., Kostyukevich S.A., Wagner T., J. Non-Cryst. Solids 266-269 (2000) 973-978
[6] Teteris J., J. Non-Cryst. Solids 299-302 (2002) 978-982

[7] Cardinal T., Richardson K.A., Shim H., Schulte A., Beatty R., Le Foulgoc K., Meneghini C., Viens J.F., Villeneuve A., J. Non-Cryst. Solids 256-257 (1999) 353-360
[8] Barney E.R., Abdel-Moneim N.S., Towey J.J., Titman J., McCarthy J.E., Bookey H.T., Kar A., Furniss D., Seddon A.B., Phys. Chem. Chem. Phys. 17 (2015) 6314 – 6327
[9] Kuzyutkina Yu. S., Romanova E. A., Kochubei V. I., Shiryaev V. S., Opt. Spectrosc. 117 (1) (2014) 49-55
[10] Knotek P., Tasseva J., Petkov K., Kincl M., Tichy L., Thin Solid Films 517 (2009) 5943–5947
[11] Todorov R., Lalova A., Petkov K., Tasseva J., Semicond. Sci. Technol. 27 (2012) 115014
[12] Musgraves J.D., Carlie N., Hu J., Petit L., Agarwal A., Kimerling L.C., Richardson K.A., Acta Mater. 59 (2011) 5032–5039
[13] Krbal M., Wagner T., Kohoutek T., Nemec P., Orava J., M. Frumar M., J. Phys. Chem. Solids 68 (2007) 953–957
[14] Kohoutek T., Wagner T., Orava J., Krbal M., Fejfar A., Mates T., Kasap S.O., Frumar M., J. Non-Cryst. Solids 353 (2007) 1437–1440
[15] Pálka K., Syrový T., Schröter S., Brückner S., Rothhardt M., Vlček M., Opt. Mater. Express 4 (2) (2014) 384-395
[16] Chern G.C., Lauks I., McGhie A.R., J. Appl. Phys. 54 (1983) 4596-4601
[17] Loghina L., Palka K., Buzek J., Slang S., Vlcek M., J. Non-Cryst. Solids 430 (2015) 21-24
[18] Swanepoel R., J. Phys. E: Sci. Instrum., 16 (1983) 1214
[19] Wemple S.H., DiDomenico M., Phys. Rev. B, 3 (1971) 1338
[20] Tauc J., Mater. Res. Bull., 3 (1968) 37-46
[21] Slang S., Palka K., Loghina L., Kovalskiy A., Jain H., Vlcek M., J. Non-Cryst. Solids 426 (2015) 125–131
[22] Ston R., Vlcek Mir., Jain H., J. Non-Cryst. Solids 236 (2003) 220
[23] Pisarcik M., Koudelka L., Mater. Chem. 7 (1982) 499
[24] Holomb R., Mitsa V., Petrachenkov O., Veres M., Stronski A., Vlcek M., Phys. Status Solidi 8 (2011) 2705
[25] Ivan I., Veres M., Pocsik I., Kokeneyesi S., Phys. Status Solidi 201 (2004) 3193
[26] Han X., Tao H., Pan R., Lang Y., Shang Ch., Xing X., Tu Q., Zhao X., Phys. Procedia 48 (2013) 59 – 64
[27] Li W., Seal S., Rivero C., Lopez C., Richardson K., Pope A., Schulte A., Myneni S., Jain H., Antoine K., Miller A., J. Appl. Phys. 98 (2005) 053503
[28] Lin F., Gulbiten O., Yang Z., Calvez L., Lucas P., J. Phys. D: Appl. Phys. 44 (2011) 045404
[29] Tasseva J., Todorov R., Babeva Tz., Petkov J., J. Opt. 12 (2010) 065601
[30] Alekberov R.I., Mekhtiyeva S.I., Isayeva G., Isayev A., Semiconductors 48 (2014) 800-803
[31] Cernosek Z., Holubova J., Cernoskova E., Ruzickova A., J. Non-oxide Glas. 1 (2009) 38
[32] Daly F., Brown C., J. Phys. Chem. 77 (1973) 1859-1861
[33] Walker B.C., Agrawal R., Chem. Commun. 50 (2014) 8331
[34] Webber D.H., Buckley J.J., Antunez P.D., Brutchey R.L., Chem. Sci. 5 (2014) 2498
[35] Cook J., Slang S., Golovchak R., Jain H., Vlcek M., Thin Solid Films 589 (2015) 642–648